BIOCHEMISTRY
including biophysical chemistry & molecular biology

Article

pubs.acs.org/biochemistry

Functional Impact of a Single Mutation within the Transmembrane Domain of the Multidrug ABC Transporter Pdr5

Petra Kueppers, Rakeshkumar P. Gupta, Jan Stindt,† Sander H. J. Smits, and Lutz Schmitt*

Institute of Biochemistry, Heinrich Heine University Duesseldorf, Universitaetsstrasse 1, 40225 Duesseldorf, Germany

Supporting Information

ABSTRACT: The pleiotropic drug resistance network in budding yeast presents a first line of defense against xenobiotics, which is formed by primary and secondary active membrane transporters. Among these transporters, the ABC transporter Pdr5 is a key component, because it confers resistance against a broad spectrum of such cytotoxic agents. Furthermore, it represents a model system for homologous transporters from pathogenic fungi and has been intensively studied in the past. In addition to other mutational studies, the S1360F mutation of Pdr5 was found to modulate substrate specificity and resistance. Notably, in the S1360F background, the resistance against the immunosuppressant FK506 is drastically increased. We present a detailed analysis of this mutation that is located in the predicted cytosolic part of transmembrane helix 11. Our data demonstrate that kinetic and thermodynamic parameters of the S1360F mutant are similar to those of the wild-type protein, except for FK506-inhibited ATPase activity and the degree of competitive inhibition. In summary, our results indicate that the S1360F mutation within the transmembrane domain interferes drastically with the ability of the nucleotide-binding domains to hydrolyze ATP by interfering with interdomain crosstalk.

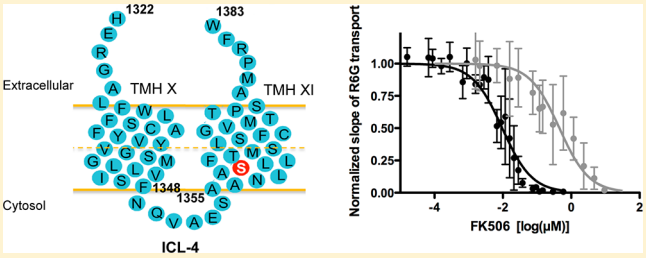

The occurrence of multidrug resistance (MDR) phenotypes is currently a major threat in medicine. Upon the treatment of cancer, bacterial infections, or fungal infections, the prolonged (or repetitive) challenge with sublethal doses of chemotherapeutics, antibiotics, or antifungal drugs, respectively, selects for more resistant cells.[1] One reason for such acquired MDR is the overexpression of plasma membrane-embedded MDR efflux pumps that actively expel a large number of cytotoxic compounds into the extracellular space.[2,3]

Drug resistance in fungi is regulated and executed by the pleiotropic drug resistance (PDR) network. Here, a battery of PDR efflux pumps under the control of PDR transcription factors acts as a first line of defense against a variety of xenobiotic compounds.[4] One of the best-studied and most abundant PDR ABC transporters in *Saccharomyces cerevisiae* is Pdr5. The remarkable degree of sequence conservation between Pdr5 and ABC transporters of clinically relevant fungi, such as *Candida albicans* and *Candida glabrata*,[5,6] makes Pdr5 a valuable model system for understanding the mechanism of multidrug transport and its inhibition in fungi.

Pdr5 consists of two nucleotide-binding domains (NBDs) and two transmembrane domains (TMDs), which represent the basic architecture of all ABC transporters.[7,8] In contrast with their general topology (TMD−NBD−TMD−NBD), a common feature of Pdr5 and its fungal homologues is an inverse arrangement of these four modules (NBD−TMD−NBD−TMD). It is now generally accepted that substrate translocation by Pdr5 and other ABC exporters is achieved by two alternating conformations that can be accessed from the inside of the cell (inward-facing conformation) or from the outside (outward-facing conformation).[9,10] Ongoing binding, hydrolysis, and product release by the NBDs provide the energetic input necessary for active transport.

The understanding of how a single protein can recognize and transport thousands of structurally and functionally diverse substrates is crucial for devising a strategy for inhibiting MDR transporters and ultimately overcoming MDR phenotypes. Numerous studies approached this by mutational analysis,[11−13] photoaffinity labeling,[14,15] cross-linking,[16−18] or substrate screens for Pdr5 and its mammalian homologue P-glycoprotein (P-gp).[19,20] The results pointed toward a polyspecific and shallow binding site. In the case of human P-gp, at least two distinct binding sites were identified (the so-called H- and R-sites). Together with these studies, the published crystal structure of mouse P-gp[21] established that transmembrane helices 5 and 6 and transmembrane helices 11 and 12 play an important role in substrate recognition.[18,22−24] In addition to the structure of mouse P-gp, the crystal structure of the putative bacterial MDR ABC transporter Sav1866 has been widely used to generate homology models of MDR ABC transporters, for which structural information is not yet available. This also includes a recently published homology model of Pdr5.[25] Nevertheless, comprehensive models that explain the dynamic processes of substrate selection, energy allocation, and transport are only starting to emerge.

Received: November 23, 2012
Revised: March 6, 2013
Published: March 6, 2013

ACS Publications © 2013 American Chemical Society

dx.doi.org/10.1021/bi3015778 | *Biochemistry* 2013, 52, 2184−2195

The occurrence of MDR phenotypes during invasive fungal infections like candidiasis or aspergillosis in immunocompromised patients[26] calls out for the identification and development of specific inhibitors of PDR efflux pumps. Theoretically, an inhibition of the drug transport activity can be achieved by competition at the stage of drug binding, by noncompetitive pump inactivation, or by the stabilization of a specific conformation locking the transporter in a nontransport competent state. Competition with drug binding was observed, for example, with second-generation inhibitors or modulators of human P-gp,[3] while third-generation inhibitors such as tariquidar seem to block P-gp function by binding to a site distinct from the actual drug binding site.[27]

A number of mostly cytotoxic or invasive agents[3] have been shown to reverse the hyper-resistance conferred by MDR ABC efflux pumps such as the immunosuppressants cyclosporin A,[28] FK506,[11] ionophore antibiotics, enniatins,[29,30] or curcuminoids.[31,32] Here, the nature of the compounds defines the exact mode of action. For instance, the immunosuppressant FK506 affects the calcineurin pathway[33,34] and inhibits Pdr5-mediated transport of several drugs.[11,35] Notably, the concise mode of transport inhibition remains unknown. In this context, the question of whether the chemosensitizer FK506 is a substrate of Pdr5 affecting drug transport by direct competition or a regulator/inhibitor acting at a site remote from the substrate binding site is still controversial. Previous studies of the impact of different substrates by Egner and co-workers identified a transmembrane mutation in Pdr5 (S1360F) that altered the substrate specificity proposing that position 1360 in Pdr5 imposes selectivity on drug recognition.[11,36]

In this study, we focus in detail on the S1360F mutation of the MDR-ABC exporter Pdr5 from *S. cerevisiae* and examine the complex interplay of substrate binding and transport modulation by FK506 in whole yeast cells and in highly enriched plasma membrane preparations. Furthermore, a detailed characterization of Pdr5 and the S1360F transmembrane mutation with respect to transport and ATPase activity in the presence and absence of the immunosuppressant FK506 and its mode of inhibition is presented. The derived data shed further light on the modulatory effect of FK506 on the interaction with Pdr5, suggesting an as yet unknown sensory function of the S1360F mutation in the crosstalk between the sites of ATP hydrolysis (NBD) and those of substrate recognition and translocation (TMD).

EXPERIMENTAL PROCEDURES

Chemicals and Yeast Strains. All chemicals were purchased from Sigma Aldrich. Stock solutions of ketoconazole (KA), fluconazole (FA), and oligomycin (OM) were prepared in dimethyl sulfoxide, and FK506 and rhodamine 6G (R6G) were dissolved in ethanol. [^{3}H]FK506 (185 GBq/mmol) and [γ-^{32}P]-8-azido-ATP (320−360 GBq/mmol) were purchased from Hartmann Analytic. Yeast was cultivated in either rich medium (YPD) or synthetic medium supplemented with appropriate auxotrophic components. In this study, *S. cerevisiae* strains *N14HISPdr5* (*MATa, ura3-52, trp1-1, leu2-3, 112 his3-11, 15, ade2-1,* Pdr1-3, N-terminal 14-histidine tag), *YHW-A5* (*MATa, ura3-52, trp1-1, leu2-3, 112, his3-11, 15, ade2-1,* Pdr1-3, *pdr5*Δ*::TRP1*), and *YRE1001* (*MATa, ura3-52, trp1-1, leu2-3, 112, his3-11, 15, ade2-1,* Pdr1-3, *pdr5, pdr5prom*Δ*::TRP1*) were used. Cloning and overexpression of the S1360F mutant were performed via site-directed mutagenesis of Pdr5 on plasmid pRE5[12] using the QuikChange II XL site-directed mutagenesis kit (Stratagene).

Liquid Drug Resistance Assay. The microdilution method was performed to determine the minimal inhibitory concentration (MIC).[37] Exponentially growing cells from a liquid YPD culture were diluted to an OD_{600} of 0.25 and used for inoculation of YPD with a constant concentration of drug and serial dilutions of FK506. Plates were incubated for 48 h at 30 °C.[11,36]

Isolation of *S. cerevisiae* Plasma Membranes. Yeast cell cultivation and isolation of plasma membranes were performed as described previously.[12,38] Cells were cultivated in YPD at 25 °C overnight with an additional supply of nitrogen and harvested at an OD_{600} of 3.5.

Sodium dodecyl sulfate−polyacrylamide gel electrophoresis (SDS−PAGE) and Western blot analysis for quality controls were performed as described previously.[12] For Western blot detection, proteins were resolved by SDS−PAGE on a 7% gel and transferred via semidry blotting to methanol-activated PVDF membranes. Whatman filters as well as the methanol-activated PVDF membranes were prepared as described previously for blotting. Membranes were incubated for at least 30 min in blocking buffer containing 3% BSA. Antiserum dilutions in blocking solutions were 1:20000 for polyclonal α-Pdr5 and 1:1000 for α-penta HIS (Qiagen) antibodies. Goat anti-rabbit (Sigma Aldrich) and goat anti-mouse (Pierce) horseradish peroxidase conjugates were used as secondary antibodies. Anti-rabbit antibodies were used at a 1:10000 dilution in TBST [20 mM Tris-HCl (pH 8.0), 250 mM NaCl, and 0.1% (w/v) Tween 20] and anti-mouse antibodies at a 1:20000 dilution in TBS buffer (TBST without Tween 20) containing 10% fat-free dry powdered milk.

R6G Transport in Whole Cells and in Isolated Plasma Membranes. Whole cell drug extrusion was measured using the method of Kolaczkowski et al.[38] with the following modifications. Equal amounts of yeast cells of exponentially growing cultures (OD_{600} = 1) were de-energized by supplementation of 5 mM 2-deoxy-D-glucose and incubated with 5 μM R6G, with or without 25 μM FK506. Identical results were obtained with 20 mM 2-deoxy-D-glucose. Therefore, all experiments were performed at a concentration of 5 mM. Cells were collected by centrifugation, washed twice with 50 mM Hepes (pH 7.0), and resuspended in this buffer. R6G efflux was initiated by addition of 20 mM glucose. Fluorescence intensities were recorded by a Fluorolog III fluorescence spectrometer (Horiba) at an excitation wavelength of 529 nm and an emission wavelength of 553 nm. Active R6G transport was performed as described previously[12] by resuspending isolated plasma membranes (20 μg) in 1 mL of transport buffer [50 mM Hepes (pH 7.0), 5 mM $MgCl_2$, 0−450 nM R6G, and 10 mM azide] and incubation at 35 °C with or without increasing amounts of FK506 prior to the initiation of transport by the addition of 10 mM ATP. Kinetic analysis of R6G fluorescence quenching was performed using Prism (version 5, GraphPad). The IC_{50} values were determined at a constant R6G concentration of 300 nM and analyzed by nonlinear regression using the general dose−response equation (eq 1):

$$Y = B_{min} + \frac{B_{max} - B_{min}}{1 + 10^{[drug] - \log IC_{50}}} \quad (1)$$

where Y represents the residual slope of the R6G fluorescence quenching, B_{min} the minimal slope, B_{max} the maximal slope, and [drug] the FK506 concentration.

dx.doi.org/10.1021/bi3015778 | *Biochemistry* 2013, 52, 2184−2195

Whole Cell Transport Assay of Radioactively Labeled FK506. Cellular transport studies were established according to accumulation assays in whole yeast cells as described previously[39] with minor modifications. Whole yeast cells were harvested from midlog phase (OD_{600} = 1) and de-energized in YP2D medium (5 mM 2-deoxy-D-glucose in YP) as a 5% cell suspension including different concentrations of [^{3}H]FK506 and FK506 in a ratio of 1:250 (total drug concentration of 0.025−40 μM) for 2 h at 30 °C to allow accumulation. Cells were collected and washed briefly four times with YP2D medium by centrifugation. One-third of the sample was separated as an internal control. The remaining cells were resuspended in YP after centrifugation and split equally, and the reaction was started by the addition of either 20 mM glucose or 5 mM 2-deoxy-D-glucose instead of glucose to take passive diffusion into account. After different times of incubation at 30 °C and while being gently shaken, the samples were rapidly harvested by centrifugation. The supernatant and the resuspended pellet in YP medium were measured upon addition of 2 mL of scintillation solution in a Beckman liquid scintillation counter (LS 3801).

Notably, in these experiments, the final concentration of FK506 was 25 μM. This is 450 times higher than the concentration required to inhibit 50% of the ATPase activity in the in vitro measurements that utilize plasma membrane preparations highly enriched in Pdr5. In intact yeast cells, however, other cellular organelles such as the vacuole effectively reduced the concentration of de facto available FK506, whose high hydrophobicity enhances this effect.

ATPase Activity Assays. Pdr5-specific ATPase activity was determined via ATPase activity measurements in the presence and absence of 20 μg/mL oligomycin. The ATPase activity measurements were taken in the presence of 4 mM ATP. Oligomycin is a specific inhibitor of the Pdr5-mediated ATPase activity.[40] The inhibitory effect of increased drug concentrations such as R6G on Pdr5-specific ATPase activity of plasma membrane fractions was measured by a colorimetric assay and performed in microtiter plates[40−42] in the presence of serial drug dilutions. K_i values were determined by fitting the data to a steady state kinetic model using a modified equation of the nonpartitioning model (eq 2) described for human P-glycoprotein (Pg-p, ABCB1):[12]

$$v = 100\left(\frac{1 - [\text{drug}]}{K_i + [\text{drug}]}\right) \quad (2)$$

Binding of [γ-^{32}P]-8-Azido-ATP to Pdr5. Photoaffinity labeling of Pdr5 was based on previously published methods.[23,43−45] Plasma membrane preparations (2.5 μg) were incubated in reaction buffer [50 mM Hepes (pH 7.0), 10 mM NaN_3, 50 mM KNO_3, 0.2 mM ammonium molybdate, and 10 mM $MgCl_2$] containing 2−10 μM [γ-^{32}P]-8-azido-ATP in a total volume of 30 μL on ice for 10 min under subdued light. Samples were cross-linked by UV illumination at 254 nm via a Stratalinker 1800 cross-linker for 8 min. The reaction was stopped by supplementation of 20 μM dithiothreitol prior to protein precipitation with 7.5% (w/v) TCA and 0.015% (w/v) sodium deoxycholate to remove excess nucleotides. The dry precipitate was resuspended in SDS sample buffer, and protein bands were separated by 7% SDS−PAGE. Photolabeling was detected by autoradiography upon exposure of the samples to Kodak Biomax Films MS/XAR at −20 °C for at least 24 h. The radioactivity incorporated was quantified by densitometry using Fujifilm MultiGauge version 3. The interaction with nonlabeled nucleotides was investigated with 5 μM [γ-^{32}P]-8-azido-ATP in the presence of increasing concentrations of ATP (0.005−4 mM) or ADP (0.01−4 mM). The analysis was performed according to nonlinear regression using the general dose−response curve described in eq 1. In this case, Y represents the extent of bound [γ-^{32}P]-8-azido-ATP, B_{min} and B_{max} stand for the corresponding minimum and maximum, respectively, and [drug] is the added ATP and ADP concentration.

Analysis of the Mode of Inhibition of FK506. R6G transport in Pdr5 wild type (WT)- or Pdr5 S1360F-containing plasma membrane vesicles was analyzed as described (see R6G Transport in Whole Cells and in Isolated Plasma Membranes). The following concentrations were used: 300, 200, 150, 75, 50, and 25 nM R6G in the presence of 0, 2, 5, 7.5, and 10 nM FK506 (Pdr5 WT) and 0, 250, 500, 750, and 1000 nM FK506 (Pdr5 S1360F). Linear slopes of the initial transport rates were determined for the 110−500 s time window and plotted as 1/slope versus 1/[R6G] (Figure 8). K_i values were determined according to the method of Dixon[46] and are summarized in Table 1.

Table 1. Summary of the Kinetic and Thermodynamic Properties of Pdr5 WT and the S1360F Mutant

	Pdr5 WT	Pdr5 S1360F
$K_{m,R6G}$ (transport) (nM)	21 ± 3	20 ± 3
$IC_{50,FK506}$ (R6G transport) (nM)	10 ± 0.1	450 ± 80
$K_{i,R6G}$ (ATPase) (μM)	0.63 ± 0.07	1.82 ± 0.17
$K_{i,FK506}$ (ATPase) (μM)	0.05 ± 0.007	4.91 ± 0.36
$IC_{50,ATP}$ (binding) (μM)	48 ± 7	51 ± 5
$IC_{50,ADP}$ (binding) (mM)	0.30 ± 0.06	0.38 ± 0.07
K_i (R6G transport by FK506) (nM)	30 ± 11	739 ± 147

RESULTS

Functional Characterization of Pdr5. Pdr5-mediated resistance toward several drugs, including steroids or azole derivatives, can be inhibited by the macrocyclic lactone FK506.[35] The S1360F mutation of Pdr5, however, represents an exception. It sustains drug resistance in the presence of the immunosuppressant FK506, an effect that was first described by Egner et al.[11] According to a hydrophobicity analysis, residue 1360 is located in the intracellular part of putative transmembrane helix 11 (TMH 11) of Pdr5 (Figure 1A). This prediction is in agreement with the homology structure of Pdr5.[25] TMH 11 follows the fourth intracellular loop (ICL-4) corresponding to the second intracellular coupling helix, which interacts in trans with the X-loop of the second NBD in the crystal structure of Sav1866[47] and in the homology model of Pdr5. Additionally, TMH 11 seems to form an amphipathic α-helix (Figure 1B), in which the hydrophobic face is positioned toward the lipid bilayer. In such an alignment, the side chain of amino acid 1360 would point into the putative substrate transport pathway and a serine to phenylalanine mutation would influence the hydrophobic−hydrophilic balance. Sequence comparison with other fungal ABC transporters (Figure 1C) suggested that position 1360 is weakly conserved in fungal MDR pumps of the ABC family. With the exception of Snq2 and Cdr4, all drug exporters possess either a serine at position 1360 or a conservative exchange against threonine. In contrast, fungal ABC transporters specific for Cd^{2+} (Ycf1), bile acids (Bpt1 or Ybt1), sterol transport (Aus1), or the export of the a-

dx.doi.org/10.1021/bi3015778 | Biochemistry 2013, 52, 2184−2195

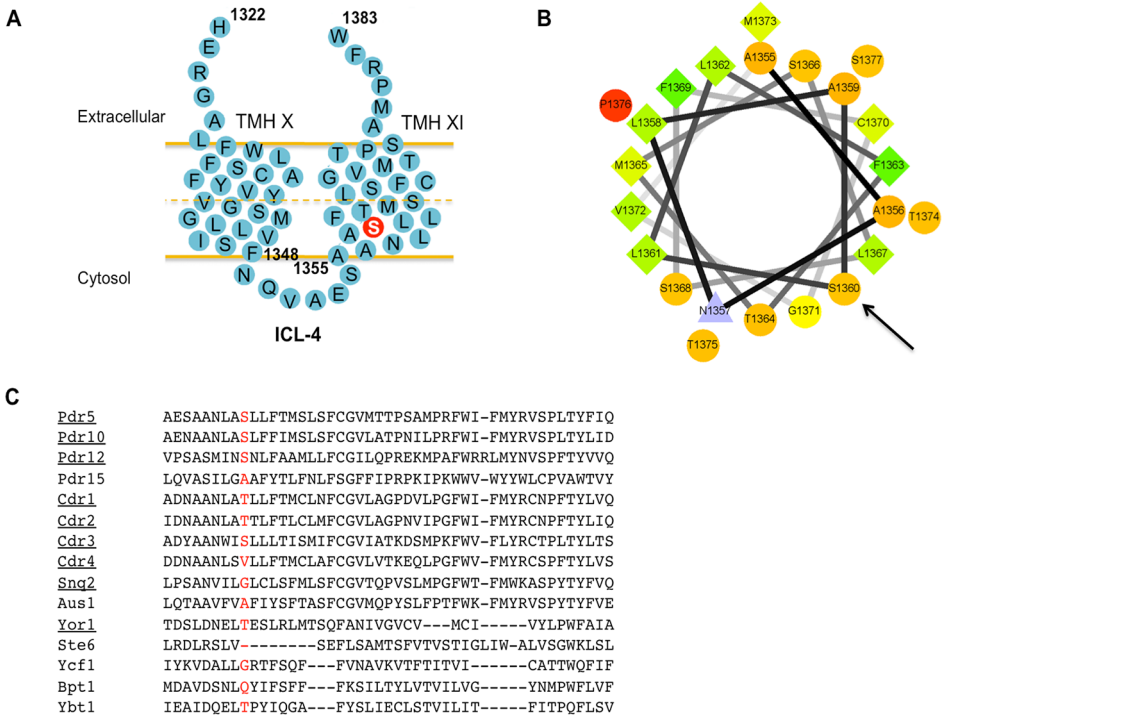

Figure 1. In silico analysis of amino acids 1322−1383 of Pdr5. (A) Predicted membrane topology of residues 1322−1383 of Pdr5 harboring putative TMH 10 and TMH 11. According to this model, residue 1360 (colored red) is localized in TMH 11. (B) Helical wheel projection of residues 1355−1377 forming TMH 11. Green and yellow diamonds represent hydrophobic residues and orange circles hydrophilic residues; the magenta triangle represents a polar, noncharged residue and the red circle a proline residue. (C) Sequence alignment of putative TMH 11 of Pdr5 with different fungal ABC transporters. Residue 1360 of Pdr5 and the other fungal ABC transporters is colored red. Fungal MDR ABC transporters are underlined.

factor (Ste6) do not contain a serine or threonine residue at the corresponding position. Our observation supports the earlier notion that the region around residue 1360 is involved in drug recognition and transport.[36,48]

For a detailed functional analysis of FK506 and its interactions with Pdr5, we focused on the S1360F mutation and generated it by site-directed mutagenesis and a subsequent homologous recombination into *S. cerevisiae* strain Δ*pdr5*Δ*pdr5prom*.[12] This strain contains a mutated transcription factor *PDR1-3*, which confers constitutive expression of Pdr5. In highly enriched plasma membrane preparations of cells expressing Pdr5 WT or the S1360F mutant, similar amounts of Pdr5 were detected (Figure 2). Here, Pdr5 and the plasma membrane ATPase Pma1 appear as distinct bands in a Coomassie Blue-stained SDS−PAGE gel (Figure 2A). In PDR5 deletion strain Δ*pdr5*, no Pdr5 signal could be detected. This result was supported by Western blots using either a polyclonal anti-Pdr5 or an anti-His tag antibody (Figure 2B). This knockout strain served as a negative control in all subsequent experiments.

R6G Transport Activity of Pdr5. Real-time R6G efflux measurements in the absence or presence of the immunosuppressant FK506 were performed to analyze the transport activity of Pdr5 WT and the S1360F mutant. Drug susceptibility assays either on drug agar plates[36] or in liquid cultures (Figure S1 of the Supporting Information) in the presence of FK506 demonstrated a hypersusceptibility to the fluorescent dye R6G in Pdr5 WT-expressing cells, but not in yeast cells expressing the S1360F mutant. Real-time efflux transport assays (Figure 3) were performed as described in Experimental Procedures. Here, R6G efflux was monitored by a concentration-dependent disintegration of R6G excimers,

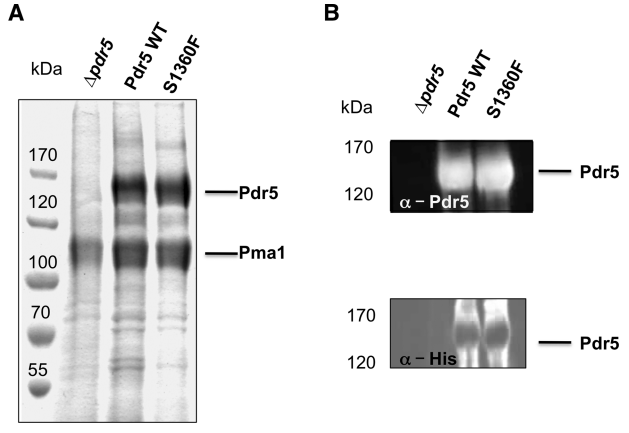

Figure 2. Expression of Pdr5 variants. (A) Coomassie Blue-stained SDS−PAGE of plasma membrane preparations of *S. cerevisiae* cells expressing no Pdr5 (Δpdr5), WT Pdr5 (Pdr5 WT), or the S1360F mutant (S1360F). Fifteen micrograms of total protein was applied per lane. Molecular masses of marker proteins are indicated at the left. Bands corresponding to Pdr5 and the plasma membrane ATPase Pma1 are indicated. (B) Western blot detection of Pdr5 variants using a polyclonal α-Pdr5 antibody (top) or a α-penta His antibody (bottom).

which results in an increase in fluorescence. In parallel, we performed two control experiments. First, H_2O was added instead of glucose to exclude diffusion effects that would increase the fluorescence. Second, deletion strain Δ*pdr5* was used to demonstrate Pdr5-dependent R6G efflux. As shown in Figure 3A, the observed changes in fluorescence intensities detected for Δpdr5 cells and the H_2O controls were minimal and therefore negligible, compared to those derived from

dx.doi.org/10.1021/bi3015778 | *Biochemistry* 2013, 52, 2184−2195

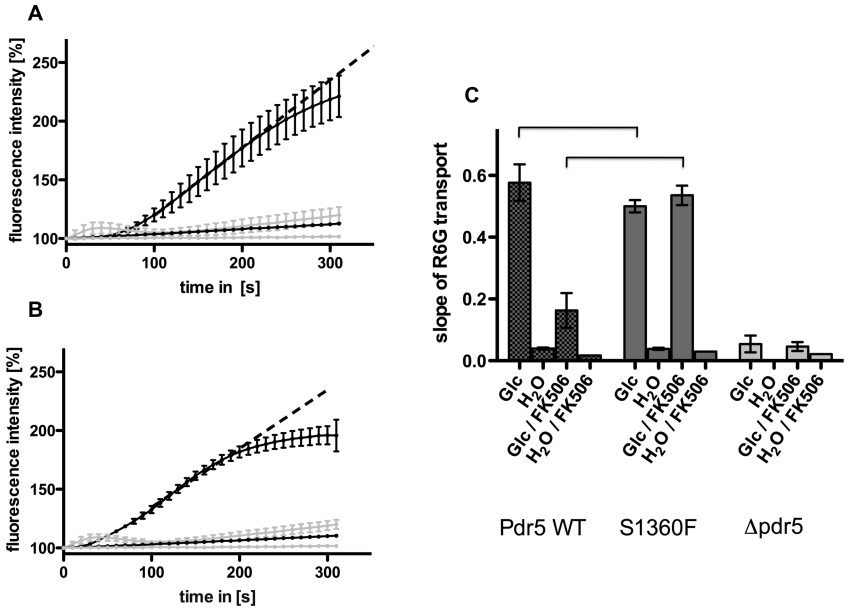

Figure 3. Whole cell drug transport. Cells were preloaded with 5 μM R6G with or without 25 μM FK506 under de-energizing conditions for 2.5 h. Twenty microliters of 1 M glucose (Glc) was added to re-energize the cells or 20 μL of H_2O as negative control at time zero. (A) Representative slope of increasing R6G fluorescence due to the export from Pdr5 WT-expressing cells after addition of glucose (■) or H_2O (□). (B) Representative slope of increasing R6G fluorescence due to the export from Pdr5 S1360F-expressing cells after addition of glucose (■) or H_2O (□). Cells lacking the *Pdr5* gene (Δ*pdr5*) were used as a negative control. Filled gray circles represent the data from the experiment conducted after energization with glucose and empty gray circles the data after addition of H_2O. (C) Rates corresponding to the slope of the linear region (dashed black line in panel A or B) of the fluorescence intensity trace. Mean values of at least three independent experiments are shown, and the error bars represent the SD.

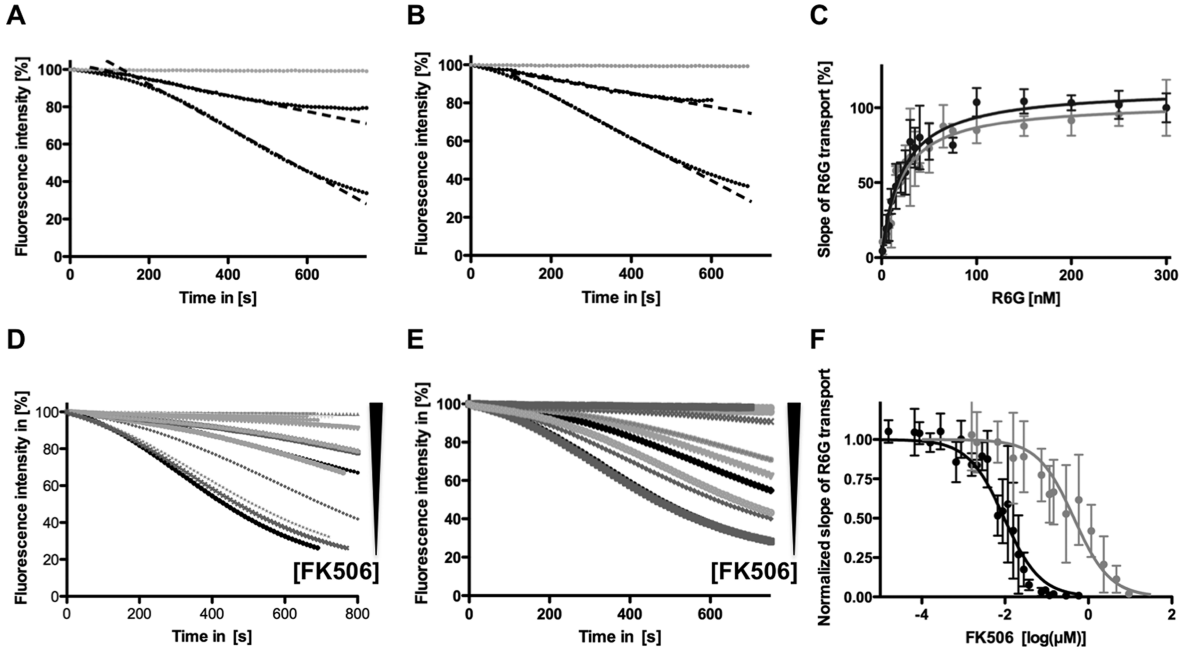

Figure 4. Kinetic characterization and inhibition of Pdr5-mediated R6G transport. (A–C) Plasma membrane preparations were incubated with different concentrations of R6G until a stable fluorescence signal was reached [roughly 300 s (trace not shown)], and the fluorescence intensity was normalized to 100%. At time zero, ATP was added. (A) Representative slopes of R6G quenching mediated by Pdr5 WT or S1360F (B) at 10 nM (top dashed line) and 300 nM R6G (bottom dashed line) as well as the negative control of plasma membrane preparations expressing no Pdr5 (gray lines) are shown. (C) Determination of K_m values for Pdr5 WT and the S1360F mutants. The rates corresponding to the linear part of the slopes for each R6G concentration were analyzed by nonlinear regression. The mean values ± SD of at least three independent experiments are plotted. (D–F) Plasma membrane preparations containing Pdr5 WT (D) or the S1360F mutant (E) were incubated with different FK506 concentrations (0–9.4 μM) in 300 nM R6G containing transport buffer prior to the addition of ATP (time zero). The recorded fluorescence intensity at time zero was normalized to 100%. (F) Analysis of the inhibitory effect of FK506 by nonlinear regression according to the general dose–response equation of R6G fluorescence quenching rates (eq 1). The derived IC_{50} values correspond to a 50% inhibition of the Pdr5-mediated R6G transport. The mean values ± SD of three to seven independent experiments are shown.

dx.doi.org/10.1021/bi3015778 | *Biochemistry* 2013, 52, 2184–2195

glucose-activated cells expressing either Pdr5 WT or the S1360F mutant (Figure 3A,B). This demonstrated that the observed R6G transport is Pdr5-dependent. To explore the impact of FK506, we determined the R6G transport rates of Pdr5 WT, the S1360F mutant, and the deletion strain in the presence and absence of FK506 under energized and de-energized conditions (Figure 3C). Transport rates in Pdr5 WT-expressing cells, which were preloaded with R6G, were reduced to 25% in the presence of FK506 as compared to the rates obtained in the absence of the immunosuppressant. An identical FK506 concentration did not affect the S1360F-mediated R6G export rate (Figure 3B,C).

To get a closer look at the mechanistic features of transport modulation by Pdr5 WT and the S1360F mutant and to test whether only structural features in the substrate-binding pocket caused the observed effect in the S1360F background, Pdr5-dependent transport of the fluorescent dye R6G was measured in isolated plasma membranes (see Experimental Procedures). Transport measurements were initiated by the addition of ATP/Mg^{2+} in the absence and presence of FK506. Here, the activation of the efflux pumps resulted in an R6G concentration-dependent formation of nonfluorescent excimers either by the redistribution of R6G within the two leaflets of the lipid bilayer in the plasma membranes or by the accumulation of R6G in inside-out plasma membrane vesicles.[38]

A comparison of the R6G transport efficiencies of Pdr5 WT and the S1360F mutant is presented in panels A and B of Figure 4 (for further details of data analysis, see Experimental Procedures). Control membranes of the deletion strain displayed no decrease in fluorescence intensity after addition of ATP. Analysis of the transport rates revealed identical Michaelis–Menten kinetics for both the wild type and the S1360F mutant (Table 1), although cells expressing the S1360F mutant exhibited an increased susceptibility to R6G compared to cells expressing Pdr5 WT in liquid cultures (data not shown) and on drug agar plates.[36] Both K_m values, for Pdr5 WT and the S1360F mutant, are in the low nanomolar range: K_m(Pdr5 WT) = 21 ± 3 nM, and K_m(S1360F) = 20 ± 3 nM (Figure 4C and Table 1). Thus, the introduction of the S1360F mutation had no apparent effect on R6G transport, suggesting that a mutation at position 1360 does not directly affect transport of this particular substrate.

As shown above, R6G transport kinetics are identical for Pdr5 WT and the S1360F mutant. However, the data derived from whole cell transport and resistance assays (Figure 3 and Figure S1 of the Supporting Information) demonstrated the abrogation of the inhibitory effect of FK506 on Pdr5-mediated R6G efflux in the background of the S1360F mutant. Therefore, we investigated R6G transport efficiencies of both the wild type and the S1360F mutant, in plasma membrane preparations in the presence of different FK506 concentrations. Already low concentrations of FK506 (0.075 μM) completely abolished R6G transport in Pdr5 WT-containing plasma membranes. In striking contrast, membranes containing Pdr5 S1360F still displayed around 40% transport activity compared to the fluorescence quenching rates in the absence of FK506. Determination of the IC_{50} values according to eq 1 revealed an almost 50-fold difference between Pdr5 WT (IC_{50} = 10 ± 0.1 nM) and the S1360F mutant (IC_{50} = 450 ± 80 nM) (Figure 4F and Table 1). Compared to whole cell transport measurements, efflux data obtained for plasma membrane preparations demonstrated that FK506 also influenced the transport efficiency of the S1360F mutant. Hence, the FK506 concentration used in the whole cell assay was not sufficient to cause an effect on the ability of the S1360F mutant to export R6G. Nevertheless, the derived transport data in plasma membrane preparations (Figure 4E,F) clearly displayed an involvement of FK506 in R6G transport modulation in the S1360F background. Most importantly, both transport assays confirmed that S1360F and Pdr5 WT display identical R6G transport parameters in the absence of FK506. Taken together, these results raised the question about the function of the S1360F mutation in FK506 transport modulation.

Cellular Transport of Radiolabeled FK506. Egner et al. suggested that FK506 might be a substrate of Pdr5.[36] Consistent with this interpretation, drug resistance assays performed in liquid cultures indicated no susceptibility of Pdr5 WT and the S1360F mutant to concentrations of FK506 of up to 100 μM (Figure S1A of the Supporting Information). To monitor whether FK506 is actively extruded by Pdr5, the cellular transport of FK506 was investigated by incubating yeast cells with ^{3}H-labeled FK506 (100 nM at a total FK506 concentration of 25 μM) under de-energizing conditions. The amount of radioactivity in the extracellular medium as well as accumulated in cells prior to glucose supplementation was determined. In parallel, the assay was performed with 2-deoxyglucose instead of glucose. Deletion strain Δ*pdr5* served again as a negative control. As shown in Figure 5, the amount of radioactivity detected in the extracellular medium for Pdr5 WT and the S1360F mutant cells was >30% higher than in the deletion strain. Under de-energized conditions, the radioactivity measured for both Pdr5 strains was even more than 2 times lower, whereas the radioactivity obtained for the deletion strain was only slightly reduced. In summary, these data demonstrated that Pdr5 actively exports FK506 and that FK506 is indeed a substrate of Pdr5.

Furthermore, the time dependencies of FK506 transport by Pdr5 WT and the S1360F mutant were determined to address the question of whether the observed inhibitory effect of FK506 on Pdr5-mediated R6G transport (Figures 3 and 4) might be due to changes in the overall transport efficiency. For this purpose, the efficiencies of transport of FK506 by Pdr5 WT and the S1360F mutant were compared at 25 μM FK506 (final concentration containing 100 nM ^{3}H-labeled FK506). This corresponds to the inhibitory conditions of R6G transport in whole yeast cells (see above). The time courses for Pdr5 WT- and S1360F-overexpressing cells were identical (Figure 5B, ii). Moreover, the application of drug at lower and higher concentrations led to comparable results for the time dependence of FK506 transport of both strains (Figure 5B, i–iv). The same held true for the slopes of Pdr5 WT- and S1360F-mediated FK506 transport. In addition, the susceptibility assays in liquid cultures with increasing FK506 concentrations revealed identical resistance patterns of both strains (Figure S1A of the Supporting Information). Taken together, these results demonstrated that Pdr5 WT and the S1360F mutant transport FK506 in a similar if not identical manner.

Pdr5-Specific ATPase Activity in the Presence of Drugs. The reported transport studies (Figures 3–5) prompted us to perform a thorough comparison of ATPase activities of Pdr5 WT and S1360F in the hope of obtaining a better mechanistic understanding of this mutation. Hence, the substrate-induced effects on the Pdr5-specific ATPase activity in the presence of R6G or FK506 were analyzed (Figure 6). Pdr5 WT[12] as well as the S1360F mutant displayed a high basal

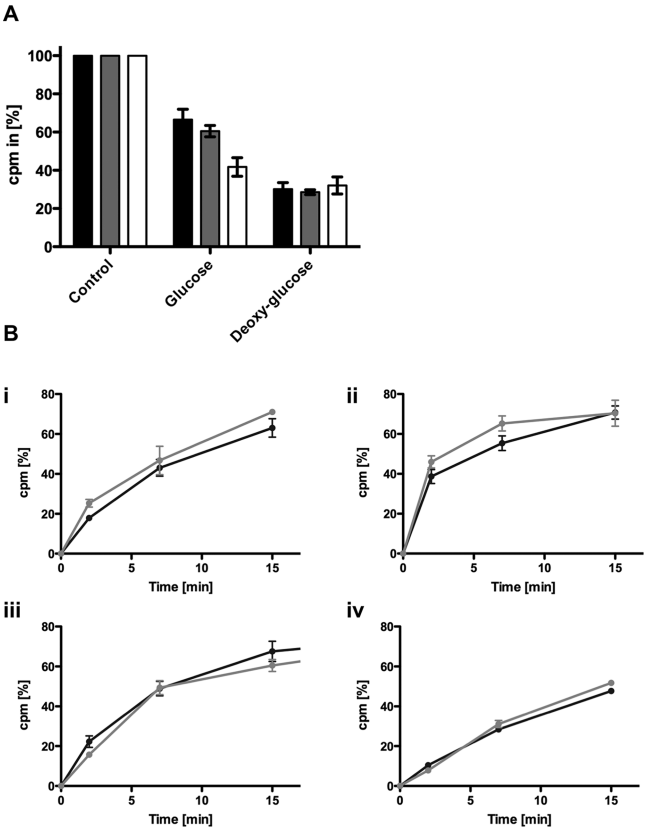

Figure 5. Cellular [^{3}H]FK506 transport. (A) Radioactive FK506 transport in yeast. Cells were incubated with 25 μM FK506 (100 nM [^{3}H]FK506) under de-energizing conditions for 2 h at 30 °C while being constantly shaken. One-third of the cells served as an internal control, and the radioactivity measured was set to 100%. The remaining two-thirds were split equally for transport measurements, and the reaction was started by the addition of 20 mM glucose or 5 mM 2-deoxyglucose as a negative control. The radioactivity in the supernatant was detected after incubation for 15 min at 30 °C and displayed for Pdr5 WT (black bars) or Pdr5 S1360F (gray bars) cells. Yeast cells expressing no Pdr5 (white bars) were used as a negative control in both experiments. The mean values ± SD of at least three independent experiments are shown. (B) Time dependencies of FK506 transport into the media by yeast cells overexpressing Pdr5 WT (gray circles) or S1360F (black circles). Cells were incubated with different FK506 concentrations under de-energizing conditions: (i) 0.25, (ii) 2.5, (iii) 25, and (iv) 40 μM FK506 (as described in Experimental Procedures). The amounts of radioactive FK506 detected in the media after incubation for various times prior to glucose addition were plotted as the fractions of total [^{3}H]FK506. The mean values ± SD of an average of four independent experiments are shown.

ATPase activity with an optimum around pH 9.5 with highly similar kinetics (data not shown). Pdr5, in contrast to many other ABC transporters, is a strictly uncoupled ABC transporter; i.e., its steady state ATPase activity cannot be stimulated by substrates.[12,49] In a previous study, we demonstrated that drugs can be categorized as inhibitory or noninhibitory drugs with respect to their capacity to inhibit ATPase activity at high substrate concentrations.[12] Indeed, in the presence of high concentrations of R6G, the ATPase activity of both Pdr5 variants could be inhibited, but a 2−3-fold higher concentration of R6G was required in the case of the S1360F mutant (Figure 6A). However, analysis of the FK506-mediated inhibition of the basal ATPase activity of both Pdr5 WT and the S1360F mutant revealed even more striking differences. To achieve 50% inhibition of the basal ATPase activity, 4.9 ± 0.4 μM FK506 was required in the case of the S1360F mutant, while 50% inhibition of Pdr5 WT ATPase was achieved when using only 0.05 ± 0.007 μM FK506. Thus, an almost 100-fold difference in the functional response of the S1360F mutant was observed (Figure 6B and Table 1).

Nucleotide Binding Properties. Drug translocation and transport modulation require an intense crosstalk between the TMDs and the allocation of energy in the NBDs.[23] An obvious prerequisite for energy allocation and coupling is the binding and hydrolysis of ATP as well as the subsequent release of ADP at the NBDs. In Pdr5, the S1360F mutation located in the TMD might induce alterations in the affinity of the NBDs for nucleotides in Pdr5 as described, for example, for mutations in P-gp.[23,50,51] Therefore, we analyzed the impact of the S1360F mutation on the nucleotide binding properties of Pdr5 WT and the S1360F mutation employing the photoactive nucleotide analogue [γ-^{32}P]-8-azido-ATP in the presence of increasing concentrations of nonlabeled ATP and ADP (Figure 7). The assay was performed at 4 °C to prevent ATP hydrolysis (see Experimental Procedures). Additional competition studies using varying ATP and ADP concentrations were performed with saturating concentrations of [γ-^{32}P]-8-azido-ATP (5 μM). An analysis of the dose-dependent displacement of [γ-^{32}P]-8-azido-ATP binding by ATP revealed similar potencies for Pdr5 WT (IC_{50} = 48 ± 7 μM) and the S1360F mutant (IC_{50} = 51 ± 5 μM), indicating identical binding affinities of ATP for both proteins within experimental error (Figure 7A and Table 1). Additionally, competition studies using ADP to displace the nucleotide analogue also showed no significant differences of the IC_{50} values within experimental error (IC_{50} values of 0.30 ± 0.06 mM for Pdr5 WT and 0.38 ± 0.07 mM for the S1360F mutant). In summary, the binding affinities of Pdr5 WT and the S1360F mutant for both ATP and ADP are identical, indicating that nucleotide binding is not affected by this mutation. Furthermore, the affinity of ATP for Pdr5 WT and the S1360F mutant (Figure S2 of the Supporting Information) was not influenced by increasing concentrations of FK506. These findings are in line with the results of Golin et al.[44] for clotrimazole, suggesting that the FK506-mediated inhibition of ATPase activity is not due to a direct competition between the nucleotide and FK506.

Inhibition Analysis of Pdr5 WT and the S1360F Mutant. All of the investigations presented so far revealed no obvious differences between Pdr5 WT and the S1360F mutation with respect to R6G transport or ATPase activity in the absence of FK506. In clear contrast, in the presence of FK506, R6G transport, binding of nucleotides, and the ATPase activity of Pdr5 WT and the S1360F mutant displayed profound differences (Table 1). To analyze the impact of the serine to phenylalanine mutation further, we determined the type of inhibition of FK506 for Pdr5 WT and the S1360F mutation (Figure 8). As a control, we used the well-known competitive inhibitor oligomycin.[38] The IC_{50} value determined under our experimental conditions (see Experimental Procedures) was identical within experimental error to that reported by Kolaczkowski (data not shown).[38] Lineweaver−Burk analysis of R6G transport inhibition by increasing concentrations of FK506 revealed enhanced apparent K_m values, implying that FK506 is a competitive inhibitor of both Pdr5 WT and the S1360F mutant (Figure 8). In other words, FK506 binds to the same substrate-binding site as R6G. However, the

dx.doi.org/10.1021/bi3015778 | Biochemistry 2013, 52, 2184−2195

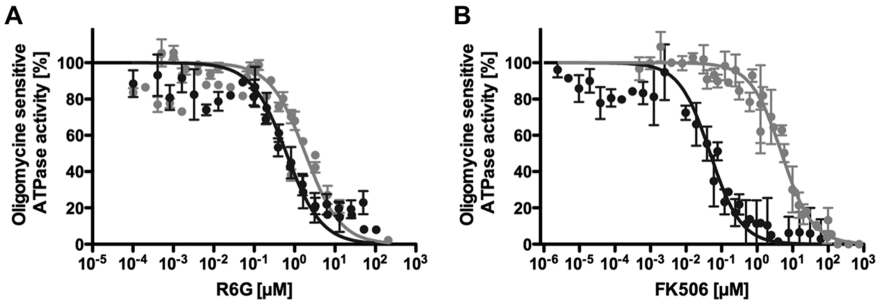

Figure 6. Concentration-dependent inhibition of Pdr5-specific ATPase activity by R6G and FK506. (A) R6G-mediated inhibition of Pdr5-specific ATPase activity of the wild type (black circles) or S1360F mutant (gray circles). (B) FK506-mediated inhibition of Pdr5-specific ATPase activity of the wild type (black circles) or S1360F mutant (gray circles). The mean values ± SD of three to seven independent experiments are shown. In both cases, the ATPase activity without added substrate was set to 100% and nonlinear regression of the data was performed according to eq 2.

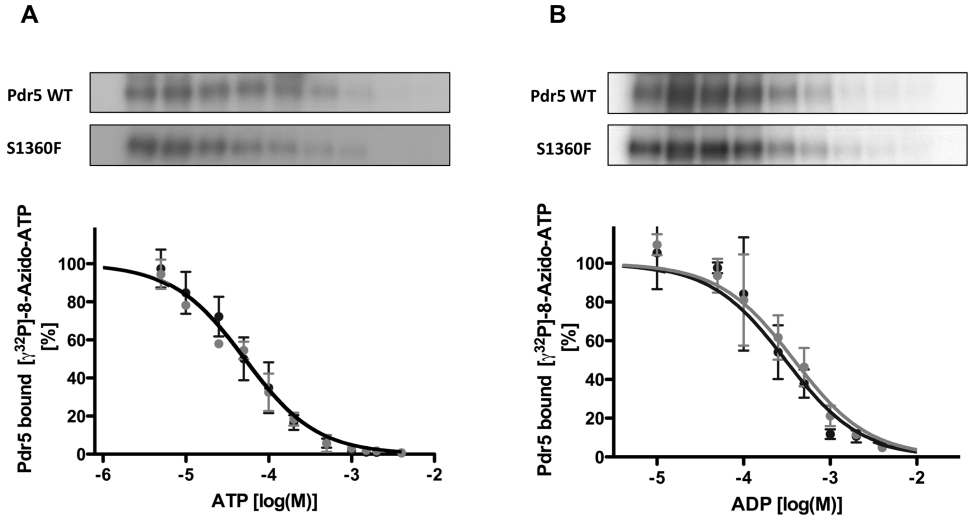

Figure 7. Nucleotide binding properties of Pdr5 and S1360F. Isolated plasma membranes of Pdr5 WT or the S1360F mutant were labeled with 5 μM [γ-^{32}P]-8-azido-ATP in the presence of nonlabeled nucleotides under nonhydrolyzing conditions as described in Experimental Procedures. (A) Displacement of [γ-^{32}P]-8-azido-ATP by increasing concentrations of ATP. The top panel shows two representative autoradiograms of Pdr5 WT or the S1360F mutant. The amount of radioactivity in the autoradiograms was analyzed by densitometry, and the extent of nucleotide binding in the absence of any nonlabeled nucleotide was set to 100%. The degree of labeling was analyzed by nonlinear regression using the general dose−response curve (eq 1). (B) Autoradiogram and analysis of the photolabeling of [γ-^{32}P]-8-azido-ATP in the presence of increasing concentrations of nonradioactive ADP for Pdr5 WT and the S1360F mutant (top). The densitometric analysis of the autoradiograms was plotted vs ATP concentration. Labeling was analyzed by nonlinear regression using the general dose−response curve (eq 1). Mean values ± SD of four independent experiments are shown for ATP or ADP displacement.

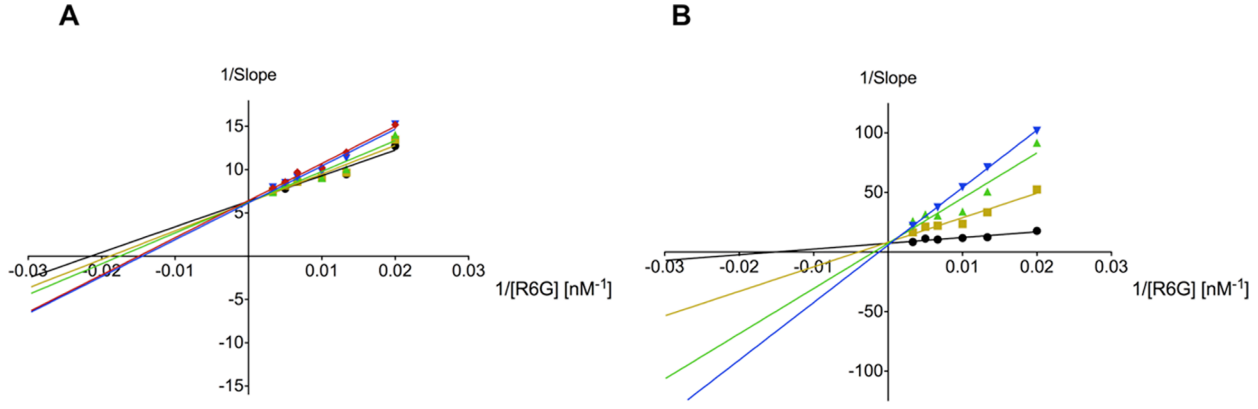

Figure 8. Inhibition of R6G transport by FK506. (A) Lineweaver−Burk analysis of R6G transport of Pdr5 WT in the presence of 0 (black), 2 (orange), 5 (green), 7.5 (blue), and 10 nM FK506 (red). (B) Lineweaver−Burk analysis of R6G transport of the S160F mutant in the presence of 0 (black), 250 (blue), 500 (green), and 750 nM FK506 (orange). Linear regression was performed using Prism version 5.0.

K_i of inhibition by FK506 increased 20-fold in the S1360F background (Table 1). This indicates that a single amino acid substitution substantially changed the nature of the substrate-binding site that R6G and FK506 occupy within Pdr5.

dx.doi.org/10.1021/bi3015778 | *Biochemistry* 2013, 52, 2184−2195

DISCUSSION

Pdr5 is the most abundant ABC transporter in yeast representing a relevant model system for fungal MDR ABC transporters. In this study, we focused on a detailed investigation of a certain mutation, S1360F, and its functional consequences for Pdr5. This missense mutation is located in putative transmembrane segment 11 (Figure 1), inside a region that displays a certain degree of conservation among fungal MDR ABC transporters from *S. cerevisiae* and *C. albicans* (Figure 1C). A specific role of the S1360F mutation in modulating antifungal resistance has been reported previously.[36,37] Substitutions of serine 1360 with different amino acids resulted in different phenotypes.[36] Interestingly, Pdr5 contains several unrelated binding sites as described by Golin et al.[52] that recognize, for instance, azoles or fluorescent dyes such as rhodamine.

In the yeast strain background used in this study, Pdr5 WT and the S1360F mutant are overexpressed to similar levels (Figure 2), allowing a quantitative comparison of the transport results (Figures 3−5), nucleotide binding, and ATPase activity measurements reported in this study. This permits a closer look at the functionality of Pdr5 WT and the S1360F mutant during the catalytic transport cycle. In addition to cell growth inhibition studies, the R6G transport data mediated by Pdr5 in vivo, especially the analysis of real-time R6G transport in vitro, demonstrated a large effect of FK506 on Pdr5's R6G transport rates (Figure 4D−F and Table 1). However, we demonstrated that the S1360F mutant displayed transport properties similar to those of Pdr5 WT in the absence of FK506. The analysis of the R6G quenching rates at different R6G concentrations revealed identical Michaelis−Menten kinetics for Pdr5 WT and the S1360F mutant with K_m values of ∼20 nM (Figure 4A−C). This suggests that S1360F does not directly participate in R6G binding. On the other hand, K_i values for FK506-mediated R6G transport inhibition of both, Pdr5 WT and the S1360F mutant differed significantly, indicating that S1360F is involved in binding of this compound (Table 1). This observation is in contrast to, for example, the transmembrane mutation S558Y in putative transmembrane helix 2 within TMD 1 of Pdr5. Here, the mutation induced a hypersensitive towards cycloheximide without affecting ATPase activity.[45] Hence, one could argue that allosteric interactions caused by the binding of FK506 are responsible for the altered R6G transport in the S1360F mutant. Such communications between multiple binding and regulatory sites have been shown, for example, for human P-gp.[51,53]

The fact that FK506 is a substrate of Pdr5 is particularly important, because the underlying mechanism of the inhibitory effect of FK506 on MDR ABC transporters is still unclear. It was reported that FK506 serves as a substrate for human P-gp.[54] Yeast cell growth inhibition studies pointed toward a similar function for Pdr5,[36] and we could show that FK506 is indeed exported by Pdr5 in an ATP-dependent fashion (Figure 5). Subsequently, the evaluation of FK506 transport characteristics of yeast cells expressing either Pdr5 WT or the S1360F mutant revealed no significant differences (Figure 5B). This is supported by the observation of identical FK506 resistance patterns in liquid drug cultures (Figure S1 of the Supporting Information) and on drug agar plates.[36] Thus, the observed loss of the inhibitory effect in the S1360F mutant is apparently not caused by changes in any FK506 transport properties.

According to the generally accepted alternating access model,[55] the process of substrate recognition and transport by the TMDs is intimately connected with the catalytic cycle of the NBDs.[56] Thus, we determined whether the mutation causes any changes in the substrate-mediated inhibition of Pdr5-specific ATPase activity to investigate the functional relevance of the S1360F mutant involved in the catalytic translocation process. Although both Pdr5 proteins (WT and S1360F) displayed almost identical K_m and v_{max} values for basal ATPase activity (data not shown), a substantial shift in the FK506-mediated inhibition of the S1360F-derived ATPase activity was observed (Figure 6B and Table 1). The K_i values differed almost 100-fold. As energy allocation in the NBDs is thought to be tightly coupled to the corresponding conformational changes in the TMDs for substrate translocation, one could expect that drastic changes in ATPase activity in the presence of a substrate are reflected in its transport properties.[12] However, in the case of FK506, such an effect was not detected. Pdr5 as well as the S1360F mutant displayed similar FK506 transport properties and susceptibilities (Figure 5B and Figure S1 of the Supporting Information), although the FK506 concentrations used exceeded the inhibitory drug concentration for Pdr5-specific ATPase activity. This observation was made on the basis of the experimental setup. While ATPase activities are measured in isolated plasma membrane preparations, radiolabeled FK506 transport is measured in whole cells, requiring much higher drug concentrations to overcome the protection barriers of the cells as well as to saturate the intracellular membranous compartments (e.g., the vacuole) that drastically lower the concentration of effectively available FK506.

In addition, displacement studies of [γ-^{32}P]-8-azido-ATP with ATP and ADP demonstrated identical nucleotide binding affinities for Pdr5 and the S1360F mutant under non-hydrolyzable conditions (Figure 7 and Table 1). Thus, changed binding affinities for these nucleotides cannot explain the observed shift in the FK506-mediated inhibition of ATPase activity between Pdr5 WT and the S1360F mutant.

However, the results obtained from liquid drug resistance assays (Figure S1 of the Supporting Information) as well as R6G transport measurements clearly demonstrated the ability of the S1360F mutation to overcome the inhibitory effect of FK506 in the presence of other substrates such as KA, FA, or R6G (Figure S1 of the Supporting Information). Moreover, the shifts in IC_{50} values to higher concentrations, as observed in both FK506-mediated ATPase and R6G transport inhibition, point to a specific role of this residue in FK506−PDR5 interactions (Figures 4F and 6B).

Further analysis revealed that FK506 is a competitive inhibitor of R6G transport in both Pdr5 WT and the S1360F mutant (Figure 8). This suggests that R6G and FK506 compete for the same binding site in Pdr5. Because R6G transport and ATPase inhibition are highly similar in the absence of FK506 for Pdr5 and the S1360F mutant (Figures 4C and 6A), these results delineate a sensory function of the S1360F mutation in FK506 transport modulation. The determined K_i of R6G transport inhibition by FK506 differed by a factor of 25 between Pdr5 WT and the S1360F mutant. The K_i of ATPase activity in the presence of FK506, however, displayed a 100-fold difference (Table 1). These significant differences lead to two conclusions. First, the affinity of Pdr5 for FK506 is increased in the S1360F background in the presence of R6G. Second and even more intriguing, the mutation actively modulates TMD−NBD communication with a pronounced effect on ATPase

activity. Because transmembrane helix 11, which harbors position 1360, is located downstream of the proposed second coupling helix observed in the crystal structure of Sav1866, such a scenario is plausible.

The identification of functionally relevant interaction partners such as amino acid residues or modulators represents an important step in elucidating the underlying mechanisms of MDR ABC transporters.[12,23,43,45] Work of Callaghan and co-workers supports the assumption that drug binding is communicated to the NBDs via distinct pathways, corroborated by an analysis of cysteine mutants in transmembrane helices 6 and 12 in P-gp.[23,43] In support of this, a modulatory communication between FK506 and the NBDs is conferred by serine 1360 and is evident by the different degree of inhibition of the ATPase activity and transport (Figures 6B and 8). In contrast to Pdr5 WT, the S1360F mutant senses the presence of FK506 differently, resulting in a stable ATPase activity as well as R6G transport, inhibition of which required larger amounts of FK506 (Figures 4F and 8). As stated above, serine 1360 is located at the interface of several potential binding sites within Pdr5,[36] of which at least three were postulated.[19,52] However, because the transport properties of Pdr5 WT and the S1360F mutant are identical (Figures 3C, 4C, and 5) and the analysis of nucleotide binding affinities showed no differences implying similar binding, hydrolysis, and release characteristics, we assume that besides thermodynamic substrate− and nucleotide−protein interactions the sensory effect of the S1360F mutation is caused by changed interprotein communications as proposed recently in the kinetic selection model.[13]

In summary, the data presented here show that a single amino acid exchange in one of the TMDs of Pdr5, S1360, has a drastic effect on substrate recognition and transport modulation by FK506. In terms of selection and transport of several substrates, this observed effect could be attributed to changes in the crosstalk of the TMDs with the NBDs and vice versa.

■ ASSOCIATED CONTENT

Ⓢ Supporting Information

Liquid drug resistance assays of Pdr5 WT and the S1306F mutant (Figure S1) and nucleotide binding in the absence or presence of FK506 of Pdr5 WT and the S1306F mutant (Figure S2). This material is available free of charge via the Internet at http://pubs.acs.org.

■ AUTHOR INFORMATION

Corresponding Author

*Institute of Biochemistry, Heinrich Heine University Duesseldorf, Universitaetsstr. 1, 40225 Duesseldorf, Germany. Phone: +49-211-81-10773. E-mail: lutz.schmitt@hhu.de.

Present Address

†J.S.: Clinic for Gasteroenterology, Hepatology and Infectiology, University Hospital Duesseldorf, Heinrich Heine University Duesseldorf, Moorenstr. 5, 40225 Duesseldorf, Germany.

Funding

This work was supported by the DFG (Grants Schm 1279/5-3 and SFB 575 Project A9) to L.S.

Notes

The authors declare no competing financial interest.

■ ACKNOWLEDGMENTS

We are indebted to Robert Ernst for essential support during the project and Karl Kuchler for stimulating discussions. We also thank Norman Nebendorf, Melanie Seidemann, Nils Hanekop, and Nacera Infed for initial support of the project and many discussions.

■ ABBREVIATIONS

ABC, ATP-binding cassette; FA, fluconazole; KA, ketoconazole; MDR, multidrug resistance; NBD, nucleotide-binding domain; OM, oligomycin; PDR, pleiotropic drug resistance; P-gp, P-glycoprotein; R6G, rhodamine 6G; SD, standard deviation; TMD, transmembrane domain.

■ REFERENCES

(1) Taubes, G. (2008) The bacteria fight back. *Science 321*, 356−361.

(2) Szakacs, G., Paterson, J. K., Ludwig, J. A., Booth-Genthe, C., and Gottesman, M. M. (2006) Targeting multidrug resistance in cancer. *Nat. Rev. Drug Discovery 5*, 219−234.

(3) Thomas, H., and Coley, H. M. (2003) Overcoming multidrug resistance in cancer: An update on the clinical strategy of inhibiting p-glycoprotein. *Cancer Control 10*, 159−165.

(4) Ernst, R., Klemm, R., Schmitt, L., and Kuchler, K. (2005) Yeast ATP-binding cassette transporters: Cellular cleaning pumps. *Methods Enzymol. 400*, 460−484.

(5) Cannon, R. D., Lamping, E., Holmes, A. R., Niimi, K., Baret, P. V., Keniya, M. V., Tanabe, K., Niimi, M., Goffeau, A., and Monk, B. C. (2009) Efflux-mediated antifungal drug resistance. *Clin. Microbiol. Rev. 22*, 291−321.

(6) Sanglard, D. (2002) Resistance of human fungal pathogens to antifungal drugs. *Curr. Opin. Microbiol. 5*, 379−385.

(7) Oswald, C., Holland, I. B., and Schmitt, L. (2006) The motor domains of ABC-transporters. What can structures tell us? *Naunyn-Schmiedeberg's Arch. Pharmacol. 372*, 385−399.

(8) Schmitt, L., and Tampe, R. (2002) Structure and mechanism of ABC transporters. *Curr. Opin. Struct. Biol. 12*, 754−760.

(9) Higgins, C. F., and Linton, K. J. (2004) The ATP switch model for ABC transporters. *Nat. Struct. Mol. Biol. 11*, 918−926.

(10) Crowley, E., and Callaghan, R. (2010) Multidrug efflux pumps: Drug binding—gates or cavity? *FEBS J. 277*, 530−539.

(11) Egner, R., Rosenthal, F. E., Kralli, A., Sanglard, D., and Kuchler, K. (1998) Genetic separation of FK506 susceptibility and drug transport in the yeast Pdr5 ATP-binding cassette multidrug resistance transporter. *Mol. Biol. Cell 9*, 523−543.

(12) Ernst, R., Kueppers, P., Klein, C. M., Schwarzmueller, T., Kuchler, K., and Schmitt, L. (2008) A mutation of the H-loop selectively affects rhodamine transport by the yeast multidrug ABC transporter Pdr5. *Proc. Natl. Acad. Sci. U.S.A. 105*, 5069−5074.

(13) Ernst, R., Kueppers, P., Stindt, J., Kuchler, K., and Schmitt, L. (2010) Multidrug efflux pumps: Substrate selection in ATP-binding cassette multidrug efflux pumps—first come, first served? *FEBS J. 277*, 540−549.

(14) Gottesman, M. M., Hrycyna, C. A., Schoenlein, P. V., Germann, U. A., and Pastan, I. (1995) Genetic analysis of the multidrug transporter. *Annu. Rev. Genet. 29*, 607−649.

(15) Kane, S. E. (1996) *Multidrug resistance of cancer cells*, Vol. *28*, pp 181−252, Academic Press, San Diego.

(16) Loo, T. W., Bartlett, M. C., and Clarke, D. M. (2004) Disulfide cross-linking analysis shows that transmembrane segments 5 and 8 of human P-glycoprotein are close together on the cytoplasmic side of the membrane. *J. Biol. Chem. 279*, 7692−7697.

(17) Loo, T. W., and Clarke, D. M. (1999) Determining the structure and mechanism of the human multidrug resistance P-glycoprotein using cysteine-scanning mutagenesis and thiol-modification techniques. *Biochim. Biophys. Acta 1461*, 315−325.

(18) Loo, T. W., and Clarke, D. M. (2000) The packing of the transmembrane segments of human multidrug resistance P-glyco-

protein is revealed by disulfide cross-linking analysis. *J. Biol. Chem. 275*, 5253−5256.
(19) Golin, J., Ambudkar, S. V., Gottesman, M. M., Habib, A. D., Sczepanski, J., Ziccardi, W., and May, L. (2003) Studies with novel Pdr5p substrates demonstrate a strong size dependence for xenobiotic efflux. *J. Biol. Chem. 278*, 5963−5969.
(20) Golin, J., Barkatt, A., Cronin, S., Eng, G., and May, L. (2000) Chemical specificity of the PDR5 multidrug resistance gene product of *Saccharomyces cerevisiae* based on studies with tri-n-alkyltin chlorides. *Antimicrob. Agents Chemother. 44*, 134−138.
(21) Aller, S. G., Yu, J., Ward, A., Weng, Y., Chittaboina, S., Zhuo, R., Harrell, P. M., Trinh, Y. T., Zhang, Q., Urbatsch, I. L., and Chang, G. (2009) Structure of P-glycoprotein reveals a molecular basis for poly-specific drug binding. *Science 323*, 1718−1722.
(22) Ueda, K., Taguchi, Y., and Morishima, M. (1997) How does P-glycoprotein recognize its substrates? *Semin. Cancer Biol. 8*, 151−159.
(23) Crowley, E., O'Mara, M. L., Reynolds, C., Tieleman, D. P., Storm, J., Kerr, I. D., and Callaghan, R. (2009) Transmembrane helix 12 modulates progression of the ATP catalytic cycle in ABCB1. *Biochemistry 48*, 6249−6258.
(24) Crowley, E., McDevitt, C. A., and Callaghan, R. (2010) Generating inhibitors of P-glycoprotein: Where to, now? *Methods Mol. Biol. 596*, 405−432.
(25) Rutledge, R. M., Esser, L., Ma, J., and Xia, D. (2011) Toward understanding the mechanism of action of the yeast multidrug resistance transporter Pdr5p: A molecular modeling study. *J. Struct. Biol. 173*, 333−344.
(26) Pfaller, M. A., and Diekema, D. J. (2007) Epidemiology of invasive candidiasis: A persistent public health problem. *Clin. Microbiol. Rev. 20*, 133−163.
(27) McDevitt, C. A., Crowley, E., Hobbs, G., Starr, K. J., Kerr, I. D., and Callaghan, R. (2008) Is ATP binding responsible for initiating drug translocation by the multidrug transporter ABCG2? *FEBS J. 275*, 4354−4362.
(28) Demeule, M., Wenger, R. M., and Beliveau, R. (1997) Molecular interactions of cyclosporin A with P-glycoprotein. Photolabeling with cyclosporin derivatives. *J. Biol. Chem. 272*, 6647−6652.
(29) Hiraga, K., Yamamoto, S., Fukuda, H., Hamanaka, N., and Oda, K. (2005) Enniatin has a new function as an inhibitor of Pdr5p, one of the ABC transporters in *Saccharomyces cerevisiae*. *Biochem. Biophys. Res. Commun. 328*, 1119−1125.
(30) Holmes, A. R., Lin, Y. H., Niimi, K., Lamping, E., Keniya, M., Niimi, M., Tanabe, K., Monk, B. C., and Cannon, R. D. (2008) ABC transporter Cdr1p contributes more than Cdr2p does to fluconazole efflux in fluconazole-resistant *Candida albicans* clinical isolates. *Antimicrob. Agents Chemother. 52*, 3851−3862.
(31) Chearwae, W., Anuchapreeda, S., Nandigama, K., Ambudkar, S. V., and Limtrakul, P. (2004) Biochemical mechanism of modulation of human P-glycoprotein (ABCB1) by curcumin I, II, and III purified from turmeric powder. *Biochem. Pharmacol. 68*, 2043−2052.
(32) Chearwae, W., Shukla, S., Limtrakul, P., and Ambudkar, S. V. (2006) Modulation of the function of the multidrug resistance-linked ATP-binding cassette transporter ABCG2 by the cancer chemo-preventive agent curcumin. *Mol. Cancer Ther. 5*, 1995−2006.
(33) Liu, J., Farmer, J. D., Jr., Lane, W. S., Friedman, J., Weissman, I., and Schreiber, S. L. (1991) Calcineurin is a common target of cyclophilin-cyclosporin A and FKBP-FK506 complexes. *Cell 66*, 807−815.
(34) Foor, F., Parent, S. A., Morin, N., Dahl, A. M., Ramadan, N., Chrebet, G., Bostian, K. A., and Nielsen, J. B. (1992) Calcineurin mediates inhibition by FK506 and cyclosporin of recovery from α-factor arrest in yeast. *Nature 360*, 682−684.
(35) Kralli, A., and Yamamoto, K. R. (1996) An FK506-sensitive transporter selectively decreases intracellular levels and potency of steroid hormones. *J. Biol. Chem. 271*, 17152−17156.
(36) Egner, R., Bauer, B. E., and Kuchler, K. (2000) The transmembrane domain 10 of the yeast Pdr5p ABC antifungal efflux pump determines both substrate specificity and inhibitor susceptibility. *Mol. Microbiol. 35*, 1255−1263.
(37) Sanglard, D., Kuchler, K., Ischer, F., Pagani, J. L., Monod, M., and Bille, J. (1995) Mechanisms of resistance to azole antifungal agents in *Candida albicans* isolates from AIDS patients involve specific multidrug transporters. *Antimicrob. Agents Chemother. 39*, 2378−2386.
(38) Kolaczkowski, M., van der Rest, M., Cybularz-Kolaczkowska, A., Soumillion, J. P., Konings, W. N., and Goffeau, A. (1996) Anticancer drugs, ionophoric peptides, and steroids as substrates of the yeast multidrug transporter Pdr5p. *J. Biol. Chem. 271*, 31543−31548.
(39) Mahe, Y., Lemoine, Y., and Kuchler, K. (1996) The ATP binding cassette transporters Pdr5 and Snq2 of *Saccharomyces cerevisiae* can mediate transport of steroids in vivo. *J. Biol. Chem. 271*, 25167−25172.
(40) Decottignies, A., Kolaczkowski, M., Balzi, E., and Goffeau, A. (1994) Solubilization and characterization of the overexpressed PDR5 multidrug resistance nucleotide triphosphatase of yeast. *J. Biol. Chem. 269*, 12797−12803.
(41) Goffeau, A., and Dufour, J. P. (1988) Plasma membrane ATPase from the yeast *Saccharomyces cerevisiae*. *Methods Enzymol. 157*, 528−533.
(42) Wada, S., Niimi, M., Niimi, K., Holmes, A. R., Monk, B. C., Cannon, R. D., and Uehara, Y. (2002) *Candida glabrata* ATP-binding cassette transporters Cdr1p and Pdh1p expressed in a *Saccharomyces cerevisiae* strain deficient in membrane transporters show phosphorylation-dependent pumping properties. *J. Biol. Chem. 277*, 46809−46821.
(43) Storm, J., O'Mara, M. L., Crowley, E. H., Peall, J., Tieleman, D. P., Kerr, I. D., and Callaghan, R. (2007) Residue G346 in transmembrane segment six is involved in inter-domain communication in P-glycoprotein. *Biochemistry 46*, 9899−9910.
(44) Golin, J., Kon, Z. N., Wu, C. P., Martello, J., Hanson, L., Supernavage, S., Ambudkar, S. V., and Sauna, Z. E. (2007) Complete inhibition of the Pdr5p multidrug efflux pump ATPase activity by its transport substrate clotrimazole suggests that GTP as well as ATP may be used as an energy source. *Biochemistry 46*, 13109−13119.
(45) Sauna, Z. E., Bohn, S. S., Rutledge, R., Dougherty, M. P., Cronin, S., May, L., Xia, D., Ambudkar, S. V., and Golin, J. (2008) Mutations define cross-talk between the N-terminal nucleotide-binding domain and transmembrane helix-2 of the yeast multidrug transporter Pdr5: Possible conservation of a signaling interface for coupling ATP hydrolysis to drug transport. *J. Biol. Chem. 283*, 35010−35022.
(46) Schuetzer-Muehlbauer, M., Willinger, B., Egner, R., Ecker, G., and Kuchler, K. (2003) Reversal of antifungal resistance mediated by ABC efflux pumps from *Candida albicans* functionally expressed in yeast. *Int. J. Antimicrob. Agents 22*, 291−300.
(47) Dawson, R. J., and Locher, K. P. (2006) Structure of a bacterial multidrug ABC transporter. *Nature 443*, 180−185.
(48) Saini, P., Prasad, T., Gaur, N. A., Shukla, S., Jha, S., Komath, S. S., Khan, L. A., Haq, Q. M., and Prasad, R. (2005) Alanine scanning of transmembrane helix 11 of Cdr1p ABC antifungal efflux pump of *Candida albicans*: Identification of amino acid residues critical for drug efflux. *J. Antimicrob. Chemother. 56*, 77−86.
(49) Shukla, S., Rai, V., Banerjee, D., and Prasad, R. (2006) Characterization of Cdr1p, a major multidrug efflux protein of *Candida albicans*: Purified protein is amenable to intrinsic fluorescence analysis. *Biochemistry 45*, 2425−2435.
(50) Song, J., and Melera, P. W. (2001) Further characterization of the sixth transmembrane domain of Pgp1 by site-directed mutagenesis. *Cancer Chemother. Pharmacol. 48*, 339−346.
(51) Martin, C., Berridge, G., Mistry, P., Higgins, C., Charlton, P., and Callaghan, R. (2000) Drug binding sites on P-glycoprotein are altered by ATP binding prior to nucleotide hydrolysis. *Biochemistry 39*, 11901−11906.
(52) Golin, J., Ambudkar, S. V., and May, L. (2007) The yeast Pdr5p multidrug transporter: How does it recognize so many substrates? *Biochem. Biophys. Res. Commun. 356*, 1−5.
(53) Martin, C., Berridge, G., Higgins, C. F., Mistry, P., Charlton, P., and Callaghan, R. (2000) Communication between multiple drug binding sites on P-glycoprotein. *Mol. Pharmacol. 58*, 624−632.

(54) Saeki, T., Ueda, K., Tanigawara, Y., Hori, R., and Komano, T. (1993) Human P-glycoprotein transports cyclosporin A and FK506. *J. Biol. Chem. 268*, 6077−6080.
(55) Jardetzky, O. (1966) Simple allosteric model for membrane pumps. *Nature 211*, 969−970.
(56) Linton, K. J. (2007) Structure and function of ABC transporters. *Physiology 22*, 122−130.